Reflector features and physics consideration of the Jules Horowitz Reactor

E. PRIVAS[1], L. CHABERT
Safety and Power Plant Process
Neutronic – Shielding – Criticality Department
AREVA TA, Aix-en-Provence, France

ABSTRACT

Mechanic solicitations induced by neutrons and photons have to be featured for components lifespan determination. AREVA-TA is in charge of both the design and building on behalf of CEA of the 100 MW Jules Horowitz Reactor (JHR). This modular Material Testing Reactor is under construction in southern France, with radioisotope production and material testing capabilities. Inner core components have been designed based on mechanical and thermohydraulic considerations. Both studies require neutronic physical quantities like the neutron and photon fluxes or heat deposition. The JHR reflector outside the primary loop is composed of beryllium and gamma shield partially positioned close to the core in order to reduce photon heating on supporting aluminum structures. The design is completed and this paper is dealing with the neutronic and photonic impacts on the reflector area and on material swelling as an application.

A Monte Carlo methodology based on the MCNP code was developed to model the reactor and enhance physical quantities maps in such complex structures like the JHR reflector. Advanced meshing and options capabilities of MCNP are used and verified in this purpose. The geometry model used is very complex and well described implementing an innovative fine-tuned method for a good understanding of neutronic parameters on local structures. To reduce calculation time and enable refined meshes, biasing methods on neutrons and photons have been performed and presented. Such considerations enable a time gain of 3.5 on average when aiming at a maximum stochastic uncertainty of 2% (2σ). The radial gamma shield enables to reduce the aluminum total heating by a factor of 1.75. Spatial distribution of the gamma heating shows the importance of the interface with the surrounding area: photons and neutrons interactions close to the gamma shield create low energy photons excess, leading to higher local energy deposition at the interface. In order to keep high flux in the experimental part of the reflector, gamma shields are not continuously set around the reactor vessel. Consequently, some photon leakage arises in the reflector area, with limited impact on aluminum structures. Another physical quantity, needed to perform mechanical designs, is the flux to assess material swelling on a reflector sector. Similar to the thermal flux, the conventional flux highly depends on the reflector material. Highest values are found in the axial center core, close to high water over beryllium ratio, because of a change in the local moderator factor.

1. Introduction

Design and development of new research reactor like Material Testing Reactors (MTRs) is mainly driven by qualification of structural materials, characterization of fuel behavior during nominal conditions or accident scenarios and production of radioisotope.
In this scope, the Jules Horowitz Reactor (JHR) is intended to be a multipurpose research reactor with the largest experimental capacity in Europe [1].
One application will be to validate components both for the current nuclear reactors of second and third generation and for the future ones offering high neutron flux, both in thermal and fast range (each around 5.10^{14} $n.cm^{-2}.s^{-1}$). High experimental capability will be placed in every part of the reactor. Fuel pins and fissile samples can be charged and irradiated at the same time in the reflector area. The experimental devices, like ADELINE, MADISON or MOLFY for ^{99}Mo production are designed by CEA [2]. JHR is designed to fulfill the flux and maximum heating requirement of such experimental devices.
HORUS V2.1 [3] chained with MCNP [4] are used to compute neutronic physical quantities

[1] edwin.privas@areva.com

for thermohydraulic and mechanical analysis [5].
This paper focuses on the main reflector features and neutronic methodology. Fine flux and energy deposition distribution over the reflector will be discussed, leading to key design parameters. A mechanical application using heating and flux will be presented, showing the swelling of a sector.

2. Jules Horowitz Reactor

JHR is a 100 MW pool-type Material Testing Reactor cooled by light water. The core rack is a 60 cm height cylinder made of aluminum in which 37 drilled holes can host 34 fuel elements and 3 large devices. Every fuel assembly is composed of 8 cylindrical and concentric plates kept together with 3 stiffeners. A U_3-Si_2 metallic fuel with ^{235}U is considered within this study. A 3 cm height Al-B poisoned insert positioned 1 cm above the top of each plate aims at limiting the flux upwelling and heat deposition above the fissile zone. This is mandatory because the water is being warmer and less pressurized in this zone and the vaporization margin being lower.
7 small test locations, called ‘simple DEN’, are placed in the center of the cylindrical fuel plates in order to reach high fast flux. The others fuel elements are filled with hafnium rods to handle reactor reactivity both to provide depletion compensation and to ensure safety shutdowns. They are geometrically composed of two concentric hafnium tubes and an aluminum follower.
The core is surrounded with an aluminum vessel (containing the primary circuit) and then a reflector. The latter is mainly composed of beryllium elements, allowing a suitable thermal neutron flux for several materials tests and ^{99}Mo production.
In this paper, the experimental configuration considers 12 ADELINE devices type (called ‘PWR DEN’), consisting of UO_2 1% ^{235}U enriched fuel pin. Neutrons coming from the inner core undergo more collisions in beryllium than water reflector, with less absorption and a lower energy decrease by collision.
A zircaloy shield between core and reflector is set around half-core to reduce gamma heating in some area.
The JHR neutronic model is described on Fig 1 and Fig 2. Each reflector area is defined by a sector number and constitutes a mechanical entity. Only C1P1C6 are linked together.

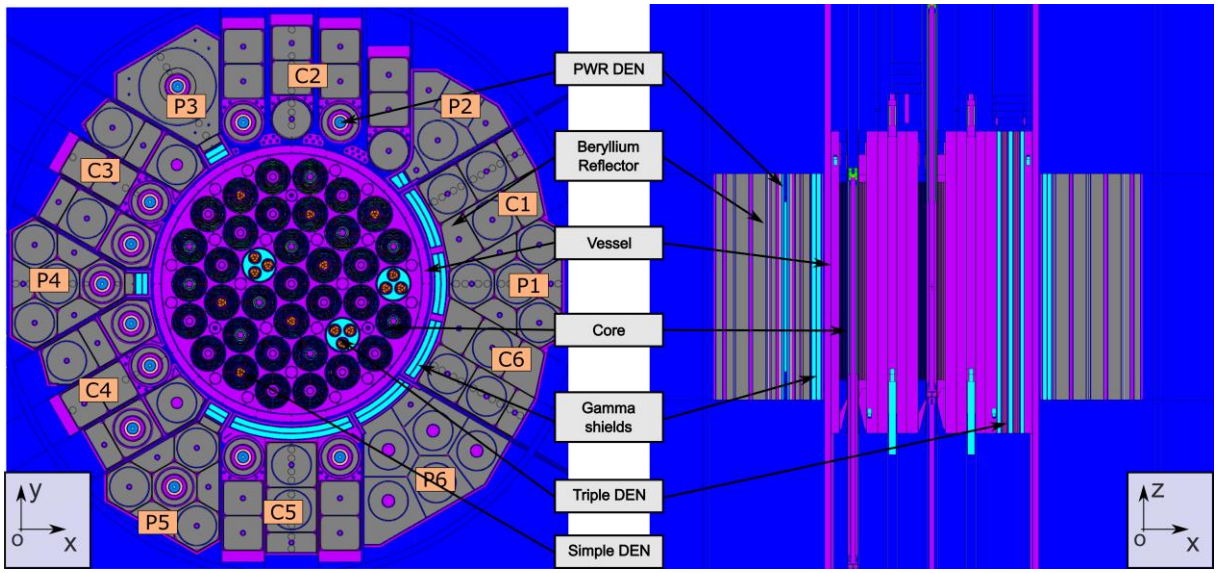

Fig 1. JHR general description. Sectors name is given within orange boxes.

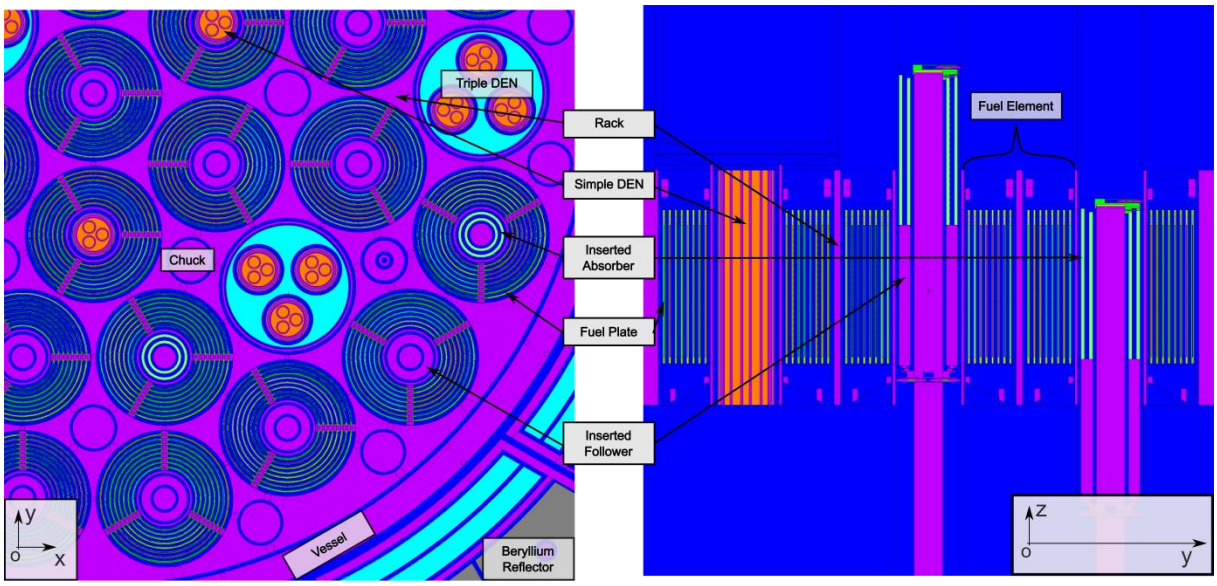

Fig 2. Core components description view

3. Neutronic computational model and methodology

Different neutronic calculation codes are available at AREVA TA to design the JHR: the determinist tools HORUS [3], the Monte Carlo transport code MCNP-6.1 [4], TRIPOLI-4® [6], Serpent-2 [7] and Geant4 [8]. The reflector design, because of its complex geometry, is performed using stochastics codes.

Moreover, MCNP is chosen because of a need to use specific options like biasing technics coupling with sur-imposed mesh. The nuclear data used in this paper is ENDF-VI.8 [9] with the photonic library coming from Lawrence Livermore Nuclear Laboratory (EPDL-92) [10].

The core and fuel burnup taken into account for this study is a Beginning Of Cycle (BOC) at equilibrium sate. The material balance comes from HORUS-V2.1 calculation scheme by simulating a build up from the first cycle to the equilibrium state, following a fuel reshuffling strategy. The average burnup at BOC is about 42 GWj/tu.

3.1 MCNP

Monte Carlo computer code, like MCNP, is a very powerful and versatile tool for particle transport calculations. It can be used for neutron and photon transport which is interesting for a reactor physicist who designs and optimizes a reactor. MCNP code is used for calculations of multiplication factor, reaction rates, neutron fluxes, power peaking factors, neutronic and gamma heating... Its main advantage is the ability to handle complex geometries. MCNP also provides multiple standard results types called “tallies”. Every output is normalized to one fission neutron in a critical calculation (using KCODE). In order to normalize the result by the thermal power of a system, scaling factors are appropriate. KCODE procedure calculation is described in section 3.2.

The “FMESH” convenient option of MCNP is used in this paper. It enables to quickly mesh an entire shape, allowing the user to describe a mesh independent of the modelled geometry and specific to the results edition. The “FMESH” card is associated to a FM card with a view to transform the flux into heat deposition. The “equivalence of F4, F6 and F7 tallies” section of the referenced manual gives more details about this use of the FM card.

3.2 Results normalization

In MCNP, the easiest way to calculate the multiplication factor and physical quantities is through KCODE card (critical calculation). Since MCNP results are normalized to one neutron fission source, they have to be properly scaled in order to get absolute comparison to the flux and total heating. The F4 and F6 tally or associated FMESH results can be scaled to a desired power level. The scaling factor is applied in data processing. The normalized factor is calculated by using directly the “loss to fission” results given in the MCNP output and the total heating in the vessel with the following formulae:

$$f_n = \frac{\mathrm{P_{Core}}}{\mathrm{C} \times \mathrm{W_{fiss}} \times \tau_f} \text{ with } \mathrm{W_{fiss}} = \mathrm{E^n_{fiss}} + \mathrm{E^\gamma_{fiss}} + \mathrm{E^\beta_{fiss}} + \mathrm{E^\gamma_{FP}}$$

With:

f_n : flux normalisation factor

$\mathrm{P_{Core}}$: core power

C : eV-J conversion factor

$\mathrm{W_{fiss}}$: energy produced per fission

τ_f : fission rate

$\mathrm{E^n_{fiss}}$: neutron heating deposited within the vessel

$\mathrm{E^\gamma_{fiss}}$: prompt gamma heating deposited within the vessel

$\mathrm{E^\beta_{fiss}}$: prompt beta heating deposited

$\mathrm{E^\gamma_{FP}}$: delayed gamma heating deposited within the vessel coming from fission product.

$\mathrm{E^n_{fiss}}$, $\mathrm{E^\gamma_{fiss}}$ and τ_f are calculated with MCNP using two FMESH containing the primary circuit. The option FM -1 0 -4 1 for gamma heating and FM -1 0 -5 -6 for neutron heating enables to get the induce energy deposition in all materials within the mesh. MCNP chosen model do not calculate directly the delayed gamma heating deposited within the vessel ($\mathrm{E^\gamma_{FP}}$). It is evaluated proportionally (b_{dg}=36%) to the prompt gamma heating ($\mathrm{E^\gamma_{fiss}}$) as:

$$\mathrm{E^\gamma_{FP}} = b_{dg} \cdot \mathrm{E^\gamma_{tot}} = b_{dg}\left(\mathrm{E^\gamma_{FP}} + \mathrm{E^\gamma_{fiss}}\right) = \frac{b_{dg}}{1-b_{dg}} \mathrm{E^\gamma_{fiss}}$$

Finally, the flux renormalisation is given by the flowing equation:

$$f_n = \frac{\mathrm{P_{Core}}}{\mathrm{C} \cdot \tau_f \left(\mathrm{E^n_{fiss}} + \mathrm{E^\beta_{fiss}} + \frac{\mathrm{E^\gamma_{fiss}}}{1-b_{dg}} \right)} = \frac{\mathrm{P_{Core}}}{\mathrm{C} \left(\mathrm{Q^n_{fiss}} + \tau_f \cdot \mathrm{E^\beta_{fiss}} + \frac{\mathrm{Q^\gamma_{fiss}}}{1-b_{dg}} \right)}$$

With:

$\mathrm{Q^n_{fiss}}$: mean neutronic heating deposited inside the vessel calculated by MCNP;

$\mathrm{Q^\gamma_{fiss}}$: mean gamma prompt heating deposited inside the vessel calculated by MCNP.

For neutron heating, the normalization factor becomes $C \cdot f_n$.

For gamma heating, the normalization factor becomes $C \cdot f_n \left(1 + b_{dg}\right)$. No nuclear data biases are considered in this paper but are taken into account for design studies.

3.3 Weighing method

With the objective to obtain finest values in the reflector area, the weight window generator capability of MCNP is chosen. The option is mandatory to converge below an uncertainty of 5% at 2σ on a fine cylindrical mesh, as describe in section 4.1.

The mesh-based weight window method developed to both increase sampling in important regions of interest and to control particle weights. Upper and lower weight bounds are assigned to each region of phase space. Particles with weights above the bounds are split so that there are more particles and their weights are within the window bounds. Particles with weights below the bounds are rouletted so that those that survive have weights increased into the window bounds. The weight bounds decrease in the direction of importance and increase away from important regions, just the opposite of importance, so that many lower weight particles are sampled in the regions of importance.

Fig 3 explains the weight window principle and shows a neutron flux weight map created by the MCNP generator.

In the JHR reflector case, the declared region of importance is located in an outside rim, in order to attract particles of interest from the inner core. More precisely, two weight maps are generated: one for fast neutron flux (>0.1 MeV) and another one for total gamma heating. For

instance, to produce the neutron weighting map, the following energy grid is taken: 0.625E-6 0.1 5 20. Those parameters were selected to:

- split very fast neutron from the core because they will contribute directly to the area of interest;
- split and deal with neutron slowdown in the reflector, for neutron between 0.1 MeV to 5 MeV;
- kill with a Russian roulette thermal neutron under 0.1 MeV;
- optimize the map to converge either on thermal flux and fast flux for different materials.

The time gained on a calculation is estimated at about 3.5, for an equivalent convergence. The weighting maps are used at different burnup steps. It is justified because the same geometry is taken into account (only control rods are withdrawn) and only one mesh is used in the core to avoid an incoherent biasing.

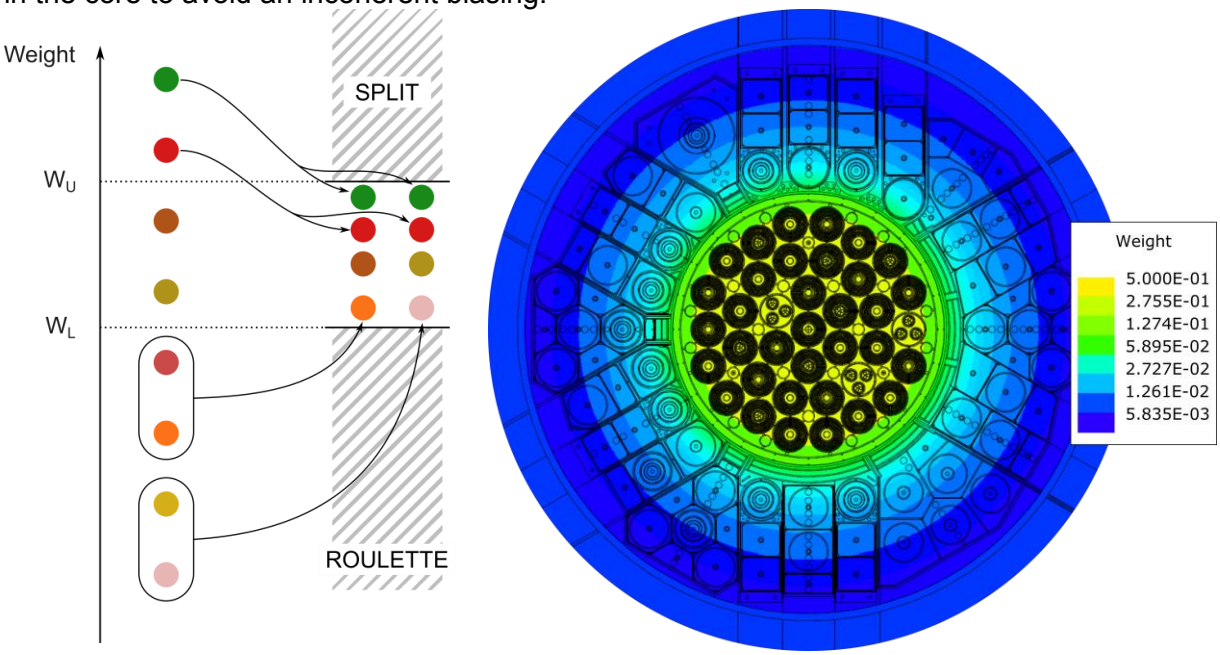

Fig 3. Weight ponderation scheme on the left and neutron flux weight map obtained with the MCNP generator on the right, for neutron energy from 5 MeV to 20 MeV

4. Discuss on neutronic results

4.1 Total heating distribution

FMESH options in MCNP are used to get neutronic and gamma heating distribution in the reflector. The fine mesh can be appreciate in Fig 4. Details are given in Tab 1.

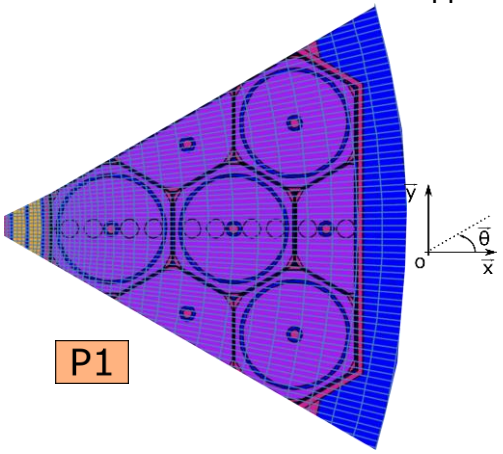

Fig 4. Fine mesh used for distribution map

Coordinate Discretization	Number of mesh
r	36
θ	720
z	10
Total	259 200

Tab 1: mesh options

FMESH is a tally flux based. It is possible to use a FM card, as described in section 3.2, to obtain neutron and photon energy deposition. Two options are commonly used: either a

virtual material for all the map, usefull for mechanical application because it is possible to interpolate correctly the physical quantities, or the FM_0 option considering effective materials. The latter option gives a good idea of the real distribution, as it can be seen on Fig 5. The neutron energy deposition is azimutaly uniform. Maximum deposition are closed to the pressure vessel, especially in the gamma shield.
Nevertheless neutron heating in reflector is, by an average factor of 5, lower than gamma heating. The effect of the gamma shield is clearly identified, with a fast decrease. It is explained because zirconium has 40 electrons, much more than other materials around, inducing much more interaction with photons. The mean efficiency of the gamma shield has been evaluated by calculating the average ratio difference between energy deposition before and after the gamma shield. This factor is about 1.75.
Fig 5. shows also the fuel pins in reflector devices (12 red points). It is explained by the fission occurring caused by a very high termal flux in those area.

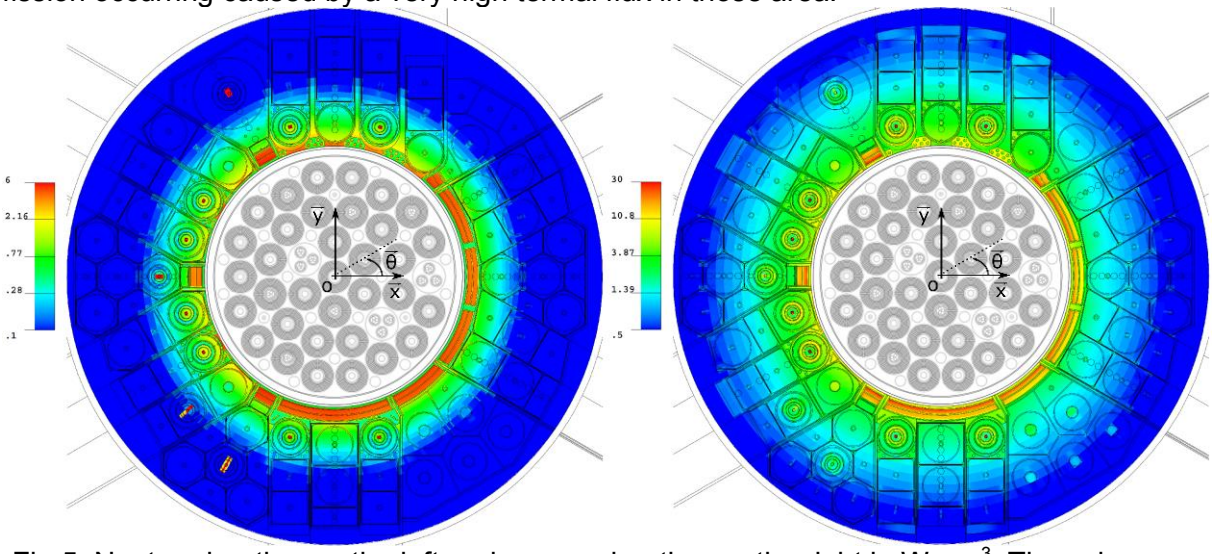

Fig 5. Neutron heating on the left and gamma heating on the right in $W.cm^{-3}$. The values are taken in the axial center of the core, integrated axially over 5 cm. Neutron heating in reflector is, by an average factor 5, lower than gamma heating (different color scale).

4.2 Focus on the gamma shield in P1

A more detailed map has been produced for gamma shield. For convenience, only the P1 is considered in this section, and more specifically along the x axis. Total heating (coming mainly from gamma energy deposited in zircaloy) is decreasing radially in the shield. Meanwhile, the exponential decrease is stopped when reaching the interface with the reflector, as shown in Fig 6. This change is explained by gamma interaction in beryllium, where Compton Effect is happening. Fig 7 shows three different curves to quantify the beryllium contribution. A first curve (in blue dot) represents the gamma spectrum in zircaloy close to the core. One can notice the electron-positron annihilation simulated by MCNP (even if no electrons have been simulated). The green curve illustrates what is happening at the shield interface with the beryllium. Finally, a simulation (orange line) with void instead of beryllium and structures shows the difference in term of contribution and how much photon is produced by Compton.

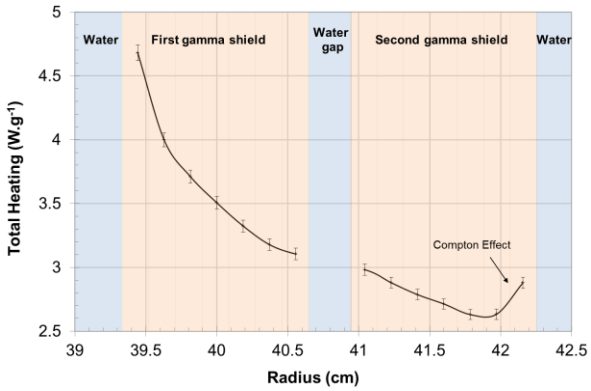

Fig 6. Total heating in the gamma shield of P1 sector (along x abscise). An increase of the energy deposition is found at the interface with the beryllium.

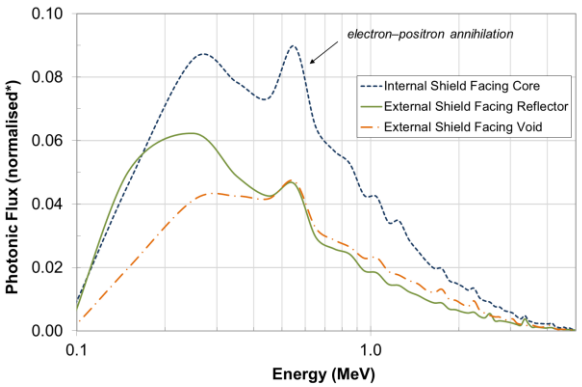

Fig 7. Photonic spectrum taken at the internal and external gamma shield interface. *Curves are normalized to the total flux of the internal shield facing core.

Similar physics and interpretations can be performed azimutaly. The main contribution is the Compton Effect coming from aluminum and photon leaks letting gamma shield borders be targeted by both core and reflector sources.

4.3 Thermal flux distribution

Fig 8 and Fig 9 show respectively the thermal flux distribution map (E<0.625 eV) and an azimuthal extract for R=38.6 cm, close to the pressure vessel. Maximum values are found in sector C2, which MOLFY samples will be held. In this area, four peaks appear and correspond to the four beryllium tables. Also, a high thermal flux is found in this location for three reasons:

- at BOC, control rods are withdrawn in this reactor part, making an artificial “balance”;
- during fuel reshuffling, fresh fuels are placed close to C2 sector;
- thin water gap after the pressure vessel contributes to efficiently slow down fast neutrons without absorbing. Meanwhile, neutrons coming back from beryllium area will mainly be capture by the water, explaining thermal flux decrease where more water is found between tables.

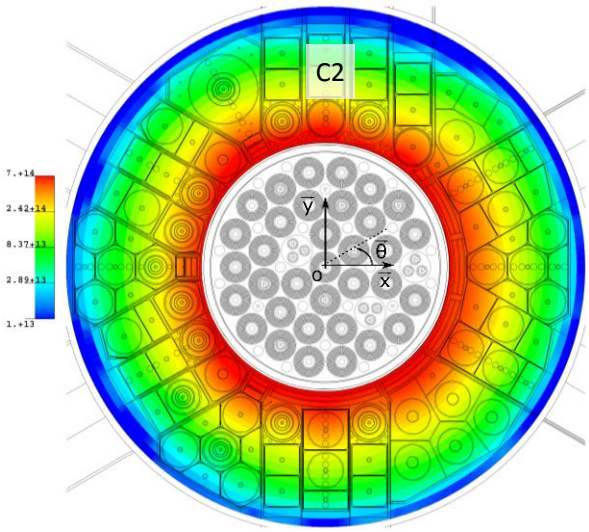

Fig 8. Thermal flux distribution. Values are taken in the axial center of the core, integrated axially over 5 cm.

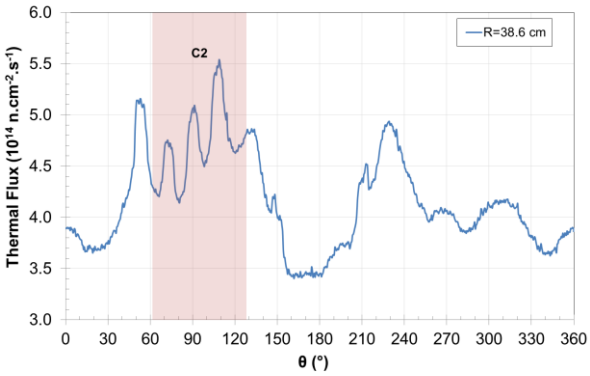

Fig 9. Azimuthal flux distribution for a radius of 38.6 cm, close to pressure vessel and crossing mainly water and aluminum structures.

5. Outlook

The previous results mentioned in this paper are supposed to be used as a dataset for mechanical studies. Then, neutronic distribution maps are interpolated over mechanical structure meshes with the use of ANSYS [11] format.

Some illustrations (Fig 10 and 11) of swelling load (coming from fluence) and total heating in P5 sector are shown based on data coming from this document. Because every sector is fixed axially at both ends, swellings will produce a deformation, given in Fig 12. This deformation has to be such that water canals are not obstructed or others structures touched. As for total heating, it may induce thermal dilatation traduced by deformations and constraints if movements are already blocked.

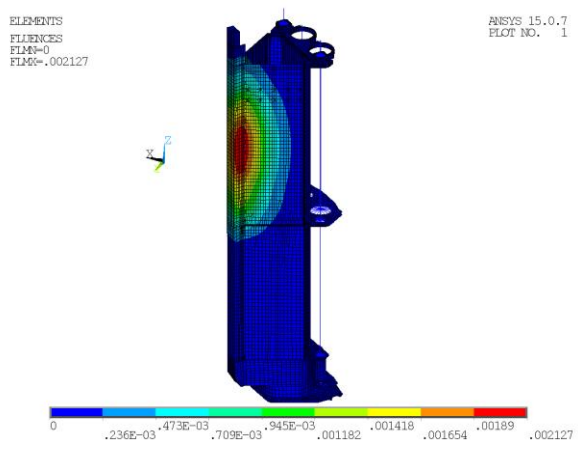

Fig 10. Swelling load in P5 triangular sector (units are in relative)

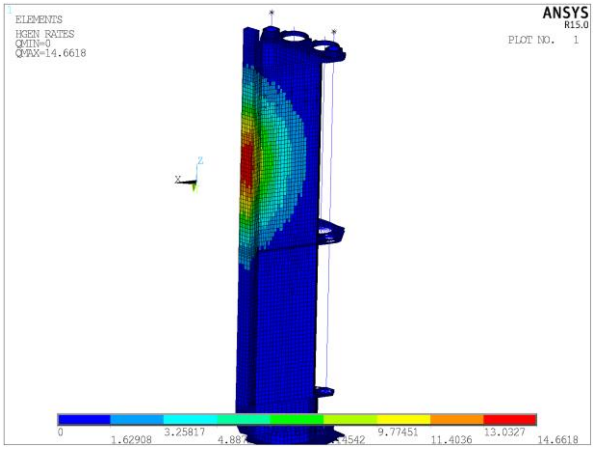

Fig 11. Thermal power due to irradiation on P5 sector (units are in W.cm^{-3})

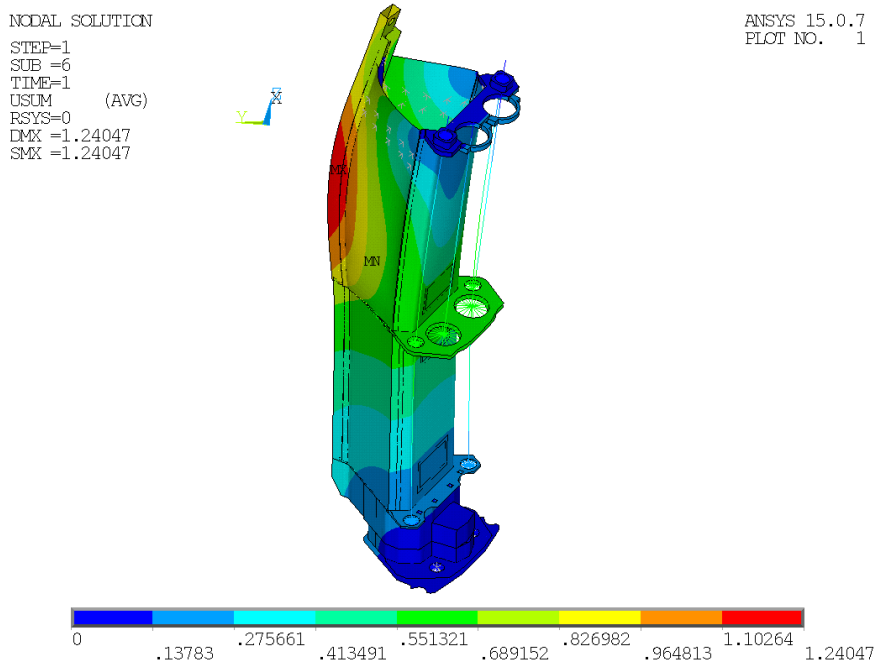

Fig 12. Induced relative movement on P5 due to swelling (units are in mm)

Further studies are foreseen between mechanic / neutronic entities, notably on the MCNP capability for reading unstructured mesh.

6. Conclusion

In a reactor design, it is mandatory to loop over different physics in order to reach the required performance. At the beginning, because of time calculation and non-obvious geometry in the JHR, simplified reflector models are requested to develop main core structures. At the end of the design, it is very important to be as close as possible to the final geometrical definition, enabling fine calculation in different fields. In this context, this paper shows the methods used in AREVA TA to answer such problematics and to link physics fields together (mostly thermohydraulic, neutronic).

Thanks to MCNP options and computer's performance, it has been possible to precisely describe the JHR neutronic reflector model, enabling to compute input data for mechanical studies such as structural swelling. Heterogeneous reflector induces specific feature on structures, like it has been seen for gamma shields. Local flux distribution is dependent on the surrounded environment. For instance, high fluctuations close to sector C2 can now be explained and dealt with.

However, in a nuclear safety approach, this step has to be confirmed with other codes. Preliminaries works has been undertaken with TRIPOLI-4®.

Further studies are lead to determine all reactor features in terms of safety and design, taking into account physical quantities variation over a cycle for example. Moreover, design studies based on photon induced heating take into account nuclear data bias thanks to high quality experimental qualification performed by CEA.

7. References

[1] G. Bignan, et al., ``The Jules Horowitz Reactor, A New high Performances European MTR (Material Testing Reactor) with modern experimental capacities: Toward an International Centre of Excellence'', Meeting of the International Group on Research Reactors (RRFM 2012), Prague, Czech Republic, March 18–22 (2012)

[2] P. Console Camprini, et al., ``Power transient analysis of fuel-loaded reflector experimental device in Jules Horowitz Reactor (JHR)'', Annals of Nuclear Energy, 94, Pages 541-554

[3] G. Willermoz, et al., ``HORUS3D : A consistent neutronics/thermohydraulics code package for the JHR modeling'', Proc. of ENC, October, 7-9, 2002, Lille, France (2002)

[4] T. Goorley, et al., ``Initial MCNP6 Release Overview'', Nuclear Technology, 180, Pages 298-315

[5] L. Chabert et al., ``Neutronic Design of small reactor'', Proceeding of the 14th. International Topical Meeting on Research Reactor and Fuel Management RRFM 2010, Marrakech (2010)

[6] O. Petit, et al., ``TRIPOLI-4 Version 8 User Guide'', Technical Report, SERMA/LTSD/RT/11-5185/A

[7] Leppänen, J., et al., ``The Serpent Monte Carlo code: Status, development and applications in 2013'', Ann. Nucl. Energy, 82, p142-150 (2015)

[8] J. Allison et al. ``Geant4 Developments and Applications'', IEEE Transactions on Nuclear Science 53 No. 1, p270-278 (2006)

[9] CSEWG-Collaboration, Evaluated Nuclear Data File ENDF/B-VI.8; Available from http://www.nndc.bnl.gov/endf

[10] H. Grady Hughes, ``Information on the MCPLIB02 Photon Library'', Los Alamos National Laboratory memorandum X-6:HGH-93-77 (January 28, 1993)

[11] ANSYS® Structural Mechanics, Release 15.0